Preclinical platform using a triple-negative breast cancer syngeneic murine model to evaluate immune checkpoint inhibitors

Nar Bahadur Bahadur (nbkatwal@chauniv.ac.kr)
CHA University College of Life Science https://orcid.org/0000-0002-7648-8044
Nahee Park
CHA University
Kamal Pandey
CHA University
Katuwal Nar Bahadur
CHA University
Min Sil Kang
CHA University
Sa Deok Hong
CHA University
Mithun Ghosh
CHA University
Seul-Gi Kim
CHA Bundang Medical Center
Young Bin Cho
CHA University
Jin Hur
CHA University
Seung Ki Kim
CHA Bundang Medical Center
Yong Wha Moon
CHA Bundang Medical Center https://orcid.org/0000-0002-7943-974X

Research Article

Keywords: TNBC (triple negative breast cancer), HR-positive, HER2-positive, PD-1 inhibitor, ICI (immune checkpoint inhibitor)

Posted Date: September 8th, 2022

DOI: https://doi.org/10.21203/rs.3.rs-1986279/v1

Abstract

Purpose

To evaluate the feasibility of syngeneic mouse models of breast cancer by analyzing the efficacy of immune checkpoint inhibitors (ICIs) and potential predictive biomarkers.

Methods

Four syngeneic mouse models of triple-negative breast cancer (TNBC) JC, 4T1, EMT6 and E0771 cells were injected subcutaneously. When the tumor reached 50–100 mm^3, each mouse model was divided into treatment (murine PD-1 antibody) and no-treatment control. Treatment group is further divided into the responder and nonresponder groups. Potential predictive biomarkers were evaluated by analyzing serum cytokines, peripheral blood T cells and tumor infiltrating immune cells.

Results

The JC model showed the highest tumor response rate (40%, 4/10) of syngeneic models: 4T1 (36%, 4/11), EMT6 (36%, 4/11), or E0771 model (23%, 3/13). Early change of tumor size at 7 days post PD-1 inhibitor treatment predicted the final efficacy of PD-1 inhibitor. Peripheral blood CD8 + and CD4 + T cells with or without Ki67 expression at 7 days post-PD-1 inhibitor treatment were higher in the finally designated responder group than in the nonresponder group. At the time of sacrifice, analyses of tumor infiltrating lymphocytes consistently supported these results. Furthermore, serum IFN-γ at 7 days post-PD-1 inhibitor treatment was also higher in responders than in nonresponders, suggesting that early changes of these markers could be predictive biomarkers of the final efficacy of ICIs.

Conclusions

Our syngeneic mouse model of TNBC is a feasible preclinical platform to evaluate ICI efficacies combined with other drugs and predictive biomarkers in the screening period of immune-oncology drug development.

Introduction

Cancer is one of the leading causes of mortality worldwide, and breast cancer is one of the most common cancers and the second leading cause of cancer-related death among women [1].

Based on the molecular marker status, estrogen receptor, progesterone receptors, and human epidermal growth factor 2 (HER2) breast cancer are classified into three major subtypes: hormone receptor (HR) positive in approximately 70% of the whole breast cancer, HER2 positive in approximately 15%, and triple

negative in approximately 15% [2]. Survival of HR-positive or HER2-positive breast cancer patients has been remarkably improved due to advance of systemic therapy, including CDK4/6 inhibitors [3] for the HR-positive subtype and various anti-HER2 therapies for the HER2-positive subtype [4]. Conversely, triple-negative breast cancer (TNBC) remains the worst prognostic disease of breast cancer subtypes due to aggressive biology and a limited number of systemic therapies [5].

However, immune checkpoint inhibitors (ICIs) have recently started to shed light on the TNBC subtype. Pembrolizumab or atezolizumab combined with standard chemotherapy as the first-line therapy has improved the progression-free survival in metastatic TNBC in the KEYNOTE 355 [6] or IMpassion 130 trials [7]. In addition, pembrolizumab combined with standard chemotherapy also enhanced the pathologic complete response and invasive disease-free survival in early TNBC in the KEYNOTE 522 trial [8]. Although these trials confirmed the PD-L1 positivity as a predictive biomarker for ICIs, several limitations regarding ICIs remain to be addressed that only a proportion of patients with TNBC shows good efficacy and PD-L1 positivity does not sufficiently predict the efficacy of ICIs. Consequently, researchers attempted to enhance the ICI efficacy in patients with TNBC and develop better predictive biomarkers.

A preclinical model to evaluate ICIs in TNBC is an urgent unmet need. Historically, syngeneic mouse models have been mainly used for immuno-oncology research based on the interaction between the murine tumor cells and a competent murine immune system [9]. However, syngeneic mouse models have several disadvantages such as not reflecting the genetic complexity of human tumors due to their lower mutational loads [10, 11]. Another disadvantage is the rapid growth of murine tumors, which do not promote the development of the chronic inflammatory environment that is characteristic of human tumors [11, 12]. Therefore, humanized mouse models, which are generated by engrafting functional human cells, tissue, or organs, have been developed to overcome disadvantages of syngeneic mouse models [13]. However, the technical complexity, the hard availability of human hematopoietic stem cells, and the high cost to establish humanized mice may limit its usage only in later stages of drug development. Therefore, the syngeneic mouse model may be a more appropriate preclinical model to potentially screen effective immunotherapies and biomarkers at the earlier stages of drug development due to its easy technique and cost-effectiveness [14].

Taken together, various TNBC syngeneic mouse models have been used to analyze the efficacy of PD-1 inhibitors and potential predictive biomarkers, with an expectation that these TNBC syngeneic mouse models could serve as a preclinical platform for screening immunotherapies along with biomarkers.

Materials And Methods

Mice and cell lines

Female BALB/c and C57BL/6 mice aged 4–6 weeks were purchased from Orient Bio Inc. (Seongnam, Korea). Mice were housed in a specific-pathogen-free animal facility at the CHA University (Seongnam, Korea). All animal experiments were approved by the Institutional Animal Care and Use Committee

(#180159) of CHA University and were performed as per the approved protocols. The mouse TNBC cell line such as 4T1, EMT6, and JC was purchased from the American Type Culture Collection (VA, USA). E0771 cell was purchased from the CH3 BioSystems (NY, USA). The cells were maintained in the Roswell Park Memorial Institute 1640 medium and supplemented with 10% fetal bovine serum (FBS) for 4T1, EMT6, and JC cells and 15% FBS for E0771 cells, and 1% penicillin/streptomycin, and were incubated at 37°C, 5% CO_2 in an incubator.

Tumor models and treatment regimens

Tumors were xenografted by subcutaneous injection of 1×10^6 4T1, EMT6, and JC cells and 5×10^5 E0771 cells into the right flank of BALB/c and C57BL/6 mice, respectively. When tumors reached 80–100 mm^3, mice were treated with either phosphate buffered saline (PBS) or anti-PD-1 monoclonal antibody (BE0188, clone J116, BioXCell, New Hampshire, USA) of 200 mg/mice by an intraperitoneal (IP) injection every 3 days up to six times. The tumor size was measured every 2 or 3 days using a caliper, and tumor volumes were calculated using the modified ellipsoid formula [$1/2 \times (\text{length} \times \text{width}^2)$]. The PD-1 inhibitor treatment group is divided into responder and nonresponder groups using the following equations:

- Responder: tumor volume in the PD-1 inhibitor treatment < mean minus standard deviation in PBS control
- Nonresponder: tumor volume in the PD-1 inhibitor treatment ≥ mean minus standard deviation in PBS control

Flow cytometric analysis of mouseperipheral blood mononuclear cell (PBMC) and tissues

Peripheral blood was collected by retro-orbital bleeding from the mice. Cells were lysed using a red blood cell (RBC) lysis buffer (eBioscience, USA) and centrifuged before collecting the PBMC layer. The tumors, spleens, and blood cells were collected from mice during the sacrifice. Tumor tissues were minced before the incubation for 1 h at 37°C with shaking in a mixture of collagenase D (1 mg/ml, Roche, Basel, Switzerland) and DNase I (10 mg/ml, Roche). Cells were suspended by repeated pipetting, filtered through a 70 μm cell strainer, and lysed to remove RBCs. After washing with PBS, suspended cells were filtered through a nylon mesh. To analyze surface markers, cells were stained with indicated antibodies. Supplementary Table S1 displays a list of antibodies. Labeled cells were obtained using a CytoFLEX flow cytometer and analyzed using FlowJo v10 (FlowJo LLC, OR, USA).

Hematoxylin and eosin (H&E) staining and immunohistochemistry (IHC)

Immune cell infiltration in the tumor was determined with IHC using 4% paraformaldehyde fixed, paraffin embedded tissues. All paraffin sections were cut at a 3 mm thickness, deparaffinized through xylene, and dehydrated with graded ethanol. For H&E staining, slides were stained with Harris hematoxylin solution and eosin Y solution. For the IHC analysis, heat-induced antigen retrieval with 0.01 M citrate buffer (pH 6.0) was used for indicated antibodies. Endogenous peroxidase activity was blocked with 3% H_2O_2 in methanol, and primary incubations were performed with mouse CD8 (1:500) or CD4 (1:500) antibodies

(Abcam, MA, USA) overnight (4°C). Subsequently, sections were incubated with secondary antibody (HRP-conjugated) for 1 h at room temperature, visualized with 3,3-diaminobenzidine tetrahydrochloride (Thermo Fisher Scientific, USA) for chromogenic development, washed, and counterstained with hematoxylin. The slides were dehydrated with graded ethanol and mounted with a Canada balsam (Junsei, Japan). To quantify IHC staining, positively stained cells were counted in five random ×400 microscopic fields for each tissue section. Five different sections were counted, and the average percentage with a standard deviation of positive cells per section was shown.

Multiplex cytokine assay

To analyze multiple mouse cytokines, approximately 75 ml of mouse blood was collected using the retro-orbital bleeding method and centrifuged for 10 min at 1,000× g. Each isolated serum sample was analyzed using the (LEGENDplex Mouse Th1 panel) bead-based immunoassay kit [including interferon (IFN)-g, tumor necrosis factor (TNF)-a, interleukin (IL)-2, IL-6, and IL-10] (BioLegend, CA, USA), according to the manufacturer's instructions. Data were obtained with a CytoFLEX flow cytometer and analyzed using LEGENDplex v8.0 software (BioLegend, CA, USA).

Statistical analysis

Statistical analyses were performed using GraphPad Prism 5.0 software (GraphPad Software, La Jolla, CA) and IBM SPSS for Windows Release 19 (SPSS Inc. Illinois, USA). Student's t-test was used to compare the tumor volume between the two groups. The analysis of variance (ANOVA) test was used to compare the immune cells, cytokines, and tumor volume among the three groups. The least significant difference (LSD) test was used for post hoc analysis. Values are represented as mean ± standard deviation unless otherwise indicated. All *p*-values were two-tailed, and *p*-values of <0.05 were considered significant.

Results

Efficacy of ICI in various TNBC syngeneic mice models

Four syngeneic mice models were produced by xenografting each mouse TNBC cell line, such as 4T1 (n = 20), E0771 (n = 16), JC (n = 20) and EMT6 cells (n = 20) (Table 1). In mice subcutaneously inoculated with indicated TNBC cells, the PD-1 inhibitor was injected six times, bleeding was performed three times, and tumors were obtained after euthanizing each mouse for profiling cytokines and immune cells as planned (Fig. 1a). Differential response to the PD-1 inhibitor was observed in four syngeneic mice models (Fig. 1b, Table 1). The JC model showed the highest tumor response rate (40%, 4/10) of syngeneic models: 4T1 (36%, 4/11), EMT6 (36%, 4/11), or E0771 model (23%, 3/13).

Table 1 Summary of outcome of efficacy of PD-1 inhibitor in syngeneic mice

Syngeneic mice model		4T1	E0771	JC	EMT6
Number of mice	Total	20	16	20	20
	Control	6	2	6	6
	PD-1i	14	14	14	14
	Total dead mice	3	1	5	13
	Dead mice (PD-1i/control)	3/0	1/0	4/1	10/3
Tumor size (mm^3) (mean ± standard deviation)	days	15 day	29 day	29 day	24 day
	Control	704±224	2571±2134	3208 ±1356	1235±452
	PD-1i	475±102	1204±743	2604±1660	1001±513
	p-value	0.01		0.25	0.20
	PD-1i/control	0.67	0.5	0.81	0.81
Response rate (n/total N) (Tumor vol < control mean-SD)		4/11 (36.3%)	3/13 (23%)	4/10 (40%)	4/11 (36.4%)

Abbreviation: PD-1i: PD-1 inhibitor, vol: volume, SD: Standard deviation

Early change of tumor size predicted final efficacy of PD-1 inhibitor treatment.

To predict the PD-1 inhibitor efficacy in TNBC syngeneic mouse model, tumor sizes were compared at early time point (7 days post PD-1 inhibitor treatment) and the final point (at the time of mice sacrifice; at 15 days for 4T1; at 29 days for E0771 and JC; at 24 days for EMT6 xenograft mice model).

In the control group 'relative tumor size' (calculated by dividing tumor size at day N by the tumor size at day 0 in each group) increased more rapidly compared to the responder group as shown in the Fig. 2a. We also analyzed the 'relative tumor size difference between responder and control group' at 7 days post PD-1 inhibitor treatment and the final day (calculated by subtracting relative tumor size at day N in control from the relative tumor size at day N in responder). In all syngeneic models, the relative tumor size differences at 7 days post PD-1 inhibitor treatment were negative numbers, suggesting that tumor response already began to appear at early time point in responders, and the relative tumor size differences became bigger at the final point (Fig. 2b). Finally, to compare relative tumor size differences among 4 syngeneic models at 7 days post PD-1 inhibitor treatment and the final day, we transformed 4 separate bar graphs from each syngeneic model in Fig. 2b into one curved-line graph (Fig. 2c). E0771 model showed that the greatest relative tumor size difference among 4 syngeneic models at 7 days post PD-1 inhibitor treatment and also the final day, whereas 4T1 model demonstrated that the smallest relative tumor size difference among 4 syngeneic models at 7 days post PD-1 inhibitor treatment and also the final day. JC and EMT6 models showed moderate relative tumor size difference both at 7 days post PD-1 inhibitor treatment and the final day. Accordingly, relative tumor size difference at early point (7 days post PD-1 inhibitor injection) predicted the final difference of relative tumor size at sacrifice, which suggests change of tumor size at 7 days post PD-1 inhibitor treatment can be an early biomarker of final efficacy of PD-1 inhibitor in our preclinical model.

Early biomarkers using peripheral blood T cells for the PD-1 inhibitor efficacy

It may be very advantageous that we can identify predictive biomarkers for ICI efficacy at an earlier time. Therefore, we further investigated peripheral blood mononuclear cell markers at 7 days post-PD-1 inhibitor treatment to correlate the final efficacies of the PD-1 inhibitor in each syngeneic mouse model. Collected blood samples were stained with T cell markers, such as CD8+ and CD4+ T cells and proliferation marker Ki67 and analyzed by flow cytometry. Fig. 3a shows the gating strategy for flow cytometry analysis.

At 7 days post-PD-1 inhibitor treatment, earlier changes in the proportion of CD4+ and CD8+ T cells in the peripheral blood are shown in Fig. 3b. Representatively in the JC model, CD8+ T cells were 3.2-fold higher in responders compared to PBS treatment control (ANOVA, p =0.077 among the three groups; LSD, p <0.029), and CD4+ T cells were also 2.2 fold higher in responders compared to PBS treatment control (ANOVA, p =0.066 among the three groups; LSD, p <0.038; Fig. 3b left panel). However, in the E0771 model, CD8+ or CD4+ T cells were not different among the three groups of control, responders, and nonresponders at 7 days post-PD-1 inhibitor treatment. As a proliferation marker Ki67 was incorporated in the analysis, CD8+Ki67+ T cells (11% vs. 2.5% in responders and controls, respectively; ANOVA p =0.001) and CD4+ Ki67+ T cells (24% and 10% in responders and controls, respectively; ANOVA p =0.033) were markedly increased in responders compared to PBS treatment control (Fig. 3b right panel).

Furthermore, we analyzed the early dynamic changes of CD8+, CD4+, and Ki67+ T cells from the pre-PD-1 inhibitor treatment to 7 days post-treatment based on responsiveness. In responders, CD8+Ki67+ and CD4+Ki67+ T cells were further increased in the PD-1 inhibitor treated mice at 7 days compared with pre-PD-1 inhibitor treatment (4.5-fold, p <0.001) for CD8+Ki67+ T cells and (2.5-fold, p <0.01) for CD4+Ki67+ T cells) compared to nonresponders (Fig. 3c).

Early serum cytokine changes to predict PD-1 inhibitor efficacy.

After confirming that peripheral blood CD8+, CD4+, and proliferative T cells started to increase early after a PD-1 inhibitor treatment in the responder group, we subsequently analyzed mouse serum cytokine concentrations to determine those early immunological reactions as represented by an early release of serum cytokines could predict the efficacy of PD-1 inhibitor treatment.

Fig. 4a shows the overview of how we did serum cytokine profiling in our mouse model. In order to use blood for both cytokine profiling and PBMC analysis, we collected approximately 200ul blood each time up to 3 times with retro-orbital bleeding technique. During and after the blood collection, we did not observe any adverse events in all mice, suggesting it’s a safe and reliable technique. Then, serum cytokine was analyzed by using bead-based assay, LEGENDplex, which relies upon sandwich immunoassay as shown in Fig. 4a. Thanks to the detection method of cytokines using flowcytometry, small amount of sample of 75 ml was sufficient.

Fig. 4b shows the early serum cytokine changes at 7 days post-PD-1 inhibitor treatment. Representatively in the E0771 model, the serum IFN-γ level was increased at 7 days post-PD-1 inhibitor treatment, and its expression was higher in responders compared to nonresponders (ANOVA,p =0.133 among the three groups; LSD,p =0.053) (Fig. 4b left panel). A similar expression pattern of IFN-γ was also observed in the JC model (Fig. 4b right panel). However, the TNF-α, IL-2, IL-6, and IL-10 levels did not statistically change (data not shown).

T cell infiltration in the tumor and proliferation in the spleen based on responsiveness after a PD-1 inhibitor treatment

To investigate the T lymphocyte infiltration into the tumor tissue and T cell proliferation in the spleen based on PD-1 inhibitor responsiveness, tumor tissue and spleen of E0771 syngeneic mice were analyzed by flow cytometry and IHC. Flow cytometry of tumor tissues showed a trend toward increased CD8+ and CD4+ T cells in responders compared to nonresponders (Fig. 5a left panel). Likewise, IHC analysis of infiltrated CD8+ or CD4+ T cells in tumor tissues at the time of sacrifice showed a significantly higher infiltration of CD8+ T cell (ANOVA,p =0.015 among the three groups; LSD,p < 0.019) and CD4+ T cells (ANOVA,p <0.001 among the three groups; LSD p <0.001) in responders compared to control group. Fig. 5a right panel). In the 4T1 syngeneic mouse model, we found a consistent pattern of higher tumor infiltration of CD8+ T cells in responders compared to nonresponders (Supplementary Fig. s1). Similarly, tumor IHC analysis showed that both CD8+ and CD4+ T cells were significantly higher in responders in comparison with nonresponders (ANOVA,p <0.001 among the three groups; LSD p <0.001) for CD8+ T cells and (ANOVA,p =0.016 among the three groups; LSD p =0.022) for CD4+ T cells between responders and nonresponders) (Supplementary Fig. s1b).

Regarding the T cell proliferation in the spleen by the responsiveness of PD-1 inhibitor therapy, CD4+ and CD4+Ki67+ T cells showed a trend toward a higher proportion in responders than in nonresponders (p =0.388 and p =0.588, Fig. 5b left panel). Similarly, in IHC analysis, more infiltrated CD8+ and CD4+ T cells were observed in responders compared to nonresponders by IHC (ANOVA,p =0.001 among the three groups; LSD p =0.001) for CD4+ T cells and (ANOVA,p =0.009 among the three groups; LSD p =0.007) for CD4+ T cells; Fig. 5b right panel).

Discussion

In this study, we established the protocol to evaluate the treatment effects together with an immune profile of anti-PD-1 inhibitors in syngeneic TNBC mouse models. Overall, our systematic analysis may provide valuable information for the use of syngeneic TNBC mouse models as a preclinical *in vivo* platform to evaluate the efficacy of various anticancer immunotherapies including anti-PD-1/PDL-1 inhibitors with invasive approach for biomarker analysis.

Definition of tumor response in this preclinical study, that is, “tumor volume in the PD-1 inhibitor treatment smaller than mean minus standard deviation in PBS control” is different from the tumor response in human studies based on the Response Evaluation Criteria in Solid Tumors 1.1 [15], which is

the “minimum 30% decrease in the sum of the longest diameter of target lesions.” In the mouse study, the definition of tumor response is not yet established so far. In the mouse study, particularly the syngeneic mouse study, the tumor growth rate is faster than in the human study due to the biological nature of murine tumors [11]. Therefore, we adopted a modified definition of the tumor response in this preclinical study using a syngeneic mouse model. Previous preclinical studies for ICIs demonstrated that ICIs have different tumor response rates according to different syngeneic TNBC models [16, 17]. In our preclinical study, we observed various tumor response rates, ranging from the highest (40%) in the JC model to the lowest (23%) in the E0771 model. In patients, ICI efficacies also vary based on the types of cancers or various predictive biomarkers including PD-L1, microsatellite instability (MSI)/mismatch repair deficiency (MMRd), tumor mutation burden (TMB), tumor infiltrating lymphocytes, and cytokines [18-21]. In our preclinical study, these different tumor response rates based on the syngeneic TNBC mice models may be due to different biological features in several aspects, such as tumor infiltrating lymphocytes, T cell proliferation, and cytokines just like in patients with cancer [22]. Other potential predictive biomarkers such as PD-L1, MSI/MMRd, or TMB may be tested using our preclinical model, if necessary. Researchers may choose an appropriate syngeneic TBNC model with a relatively lower response rate, to prove better efficacy of combination immunotherapy, based on our study.

It may be very advantageous that we can identify the benefits of ICIs at an earlier time. In our study, early tumor response measured at 7 days posttreatment was a good predictor of the final ICI efficacy. To the best of our knowledge, this study is the first to demonstrate this simple concept. This concept of early tumor response only by measuring the physical tumor size could be enforced with molecular imaging or multimodal imaging techniques as other researchers published [23, 24]. Furthermore, although high CD8+, CD4+, or Ki67+ T cell levels in the peripheral blood or higher serum IFN-γ concentration are well-known predictive biomarkers for ICI efficacy [25-27]. It remains unclear whether early dynamic changes of these markers could serve as predictive biomarkers for the ICI efficacy. On-treatment biomarkers during the early treatment period may become better predictive biomarkers if they are validated in clinical trials. Our preclinical model could be used to develop various on-treatment biomarkers to predict efficacy early.

Furthermore, the feasibility of our preclinical model in studying immuno-oncology drugs should be addressed. In our study, approximately 200 ul of blood was collected retro-orbitally on days 0, 7, and 27. A 200 ul volume was sufficient to perform FACS for peripheral blood immune cells or measure serum cytokines. Even better, there were no ocular complications during and post procedure, and our retro-orbital bleeding technique was considered a safe technique. Moreover, at the end of the experiments, fresh tumor tissues were collected, which was sufficient for further experiments.

The primitive limitation of the syngeneic mouse model is that translation of discoveries from mouse models to clinical trials has been hindered by various genetic and biological differences between humans and mice [28, 29]. To overcome this, the necessity of humanized mouse model was suggested [13]. However, we know that the humanized mouse model is not appropriate in the early screening period of drug development due to its low accessibility. Therefore, the syngeneic mouse model as our TNBC

preclinical model in this study is a more suitable bridging preclinical model to select in and out potential immunotherapies and biomarkers at the earlier stages of drug development.

In conclusion, we acknowledge that the syngeneic mouse model may have several limitations as mentioned above. The syngeneic mouse model has the advantage of permitting more detailed and invasive biomarker experiments. Our syngeneic mouse protocol can be used to evaluate ICI efficacies in combination with other drugs and biomarkers of immunotherapies in screening for immuno-oncology drug development.

Declarations

Author Contributions: Conceptualization, Nahee Park, Kamal Pandey, Nar Bahadur Katuwal, Seung Ki Kim, Yong Wha Moon; Data curation, Nahee Park, Kamal Pandey, Nar Bahadur Katuwal; Formal analysis, Nahee Park, Nar Bahadur Katuwal; Funding acquisition, Yong Wha Moon; Methodology, Nahee Park, Kamal Pandey, Nar Bahadur Katuwal; Project administration, Yong Wha Moon; Supervision, Seung Ki Kim, Yong Wha Moon; Validation, Yong Wha Moon; Writing original draft, Nahee Park, Nar Bahadur Katuwal; Writing review & editing, Nar Bahadur Katuwal, Yong Wha Moon. All authors have read and agreed to the published version of the manuscript.

Funding: This research was supported by two grants; one is the Korea Health Technology R&D Project through the Korea Health Industry Development Institute (KHIDI), funded by the Ministry of Health & Welfare, Republic of Korea (grant number: HI16C1559). The other one is the National Research Foundation of Korea(NRF) grant funded by the Korea government(MSIP) (No. NRF-2021R1C1C1006882).

Data Availability Statement: The dataset generated during the current study are available from the corresponding author on reasonable request.

Conflicts of interest: The corresponding author received research funds from several pharmaceutical companies including Celltrion, Boryung, Onconic Therapeutics, ImmunoMet Therapeutics, HK inno.N, and Medytox. Other authors declare no potential conflicts of interest.

Ethical approval: Ethics approval All animal experiments were approved by the Institutional Animal Care and Use Committee (IACUC, #170062) of CHA University and were carried out in accordance with the approved protocols.

Consent to publish: Not relevant

References

1. Zou Y et al (2020) Efficacy and predictive factors of immune checkpoint inhibitors in metastatic breast cancer: a systematic review and meta-analysis. Ther Adv Med Oncol 12:1758835920940928
2. Waks AG, Winer EP (2019) Breast Cancer Treatment: A Review Jama 321(3):288–300

3. Roberto M et al (2021) *CDK4/6 Inhibitor Treatments in Patients with Hormone Receptor Positive, Her2 Negative Advanced Breast Cancer: Potential Molecular Mechanisms, Clinical Implications and Future Perspectives.* Cancers (Basel), **13**(2)
4. Goutsouliak K et al (2020) Towards personalized treatment for early stage HER2-positive breast cancer. Nat Reviews Clin Oncol 17(4):233–250
5. Pralea IE et al (2020) *Mass Spectrometry-Based Omics for the Characterization of Triple-Negative Breast Cancer Bio-Signature*.J Pers Med, **10**(4)
6. Cortes J et al (2020) Pembrolizumab plus chemotherapy versus placebo plus chemotherapy for previously untreated locally recurrent inoperable or metastatic triple-negative breast cancer (KEYNOTE-355): a randomised, placebo-controlled, double-blind, phase 3 clinical trial. Lancet 396(10265):1817–1828
7. Adams S et al (2019) Atezolizumab Plus nab-Paclitaxel in the Treatment of Metastatic Triple-Negative Breast Cancer With 2-Year Survival Follow-up: A Phase 1b Clinical Trial. JAMA Oncol 5(3):334–342
8. Schmid P et al (2020) Pembrolizumab for Early Triple-Negative Breast Cancer. N Engl J Med 382(9):810–821
9. Buqué A, Galluzzi L (2018) Modeling Tumor Immunology and Immunotherapy in Mice. Trends Cancer 4(9):599–601
10. Ito M et al (2002) NOD/SCID/γ c null mouse: an excellent recipient mouse model for engraftment of human cells. Blood The Journal of the American Society of Hematology 100(9):3175–3182
11. Sanmamed M et al (2016) Defining the optimal murine models to investigate immune checkpoint blockers and their combination with other immunotherapies. Ann Oncol 27(7):1190–1198
12. Sanmamed MF, Chen L (2014) Inducible expression of B7-H1 (PD-L1) and its selective role in tumor site immune modulation. Cancer J 20(4):256
13. Park N et al (2020) *Preclinical platform for long-term evaluation of immuno-oncology drugs using hCD34 + humanized mouse model*.J Immunother Cancer, **8**(2)
14. Gould SE, Junttila MR, de Sauvage FJ (2015) Translational value of mouse models in oncology drug development. Nat Med 21(5):431–439
15. Eisenhauer EA et al (2009) New response evaluation criteria in solid tumours: revised RECIST guideline (version 1.1). Eur J Cancer 45(2):228–247
16. Barnes S et al (2015) Abstract 3362: Systematic evaluation of immune checkpoint inhibitors. Cancer Res 75(15Supplement):3362–3362
17. Taylor MA et al (2019) Longitudinal immune characterization of syngeneic tumor models to enable model selection for immune oncology drug discovery. J Immunother Cancer 7(1):328
18. Cho YA et al (2021) *PD-L1 Expression Is Significantly Associated with Tumor Mutation Burden and Microsatellite Instability Score*.Cancers (Basel), **13**(18)

19. Noh JJ et al (2021) *Frequency of Mismatch Repair Deficiency/High Microsatellite Instability and Its Role as a Predictive Biomarker of response to Immune Checkpoint Inhibitors in Gynecologic Cancers*.Cancer Res Treat,
20. Cao J et al (2022) The predictive efficacy of tumor mutation burden in immunotherapy across multiple cancer types: A meta-analysis and bioinformatics analysis. Transl Oncol 20:101375
21. Li F et al (2021) The association between CD8 + tumor-infiltrating lymphocytes and the clinical outcome of cancer immunotherapy: A systematic review and meta-analysis. EClinicalMedicine 41:101134
22. Ager EI et al (2015) *Blockade of MMP14 activity in murine breast carcinomas: implications for macrophages, vessels, and radiotherapy*.J Natl Cancer Inst, **107**(4)
23. Saida Y et al (2021) Multimodal Molecular Imaging Detects Early Responses to Immune Checkpoint Blockade. Cancer Res 81(13):3693–3705
24. Accorsi A et al (2021) Image3C, a multimodal image-based and label-independent integrative method for single-cell analysis. eLife 10:e65372
25. Huang AC et al (2017) T-cell invigoration to tumour burden ratio associated with anti-PD-1 response. Nature 545(7652):60–65
26. Zuazo M et al (2019) Functional systemic CD4 immunity is required for clinical responses to PD-L1/PD-1 blockade therapy. EMBO Mol Med 11(7):e10293
27. Zhao Q et al (2021) *Serum IL-5 and IFN-γ Are Novel Predictive Biomarkers for Anti-PD-1 Treatment in NSCLC and GC Patients.* Dis Markers, **2021**: p. 5526885
28. Hackam DG, Redelmeier DA (2006) Translation of Research Evidence From Animals to Humans. JAMA 296(14):1727–1732
29. Wang M et al (2018) Humanized mice in studying efficacy and mechanisms of PD-1-targeted cancer immunotherapy. Faseb j 32(3):1537–1549

Figures

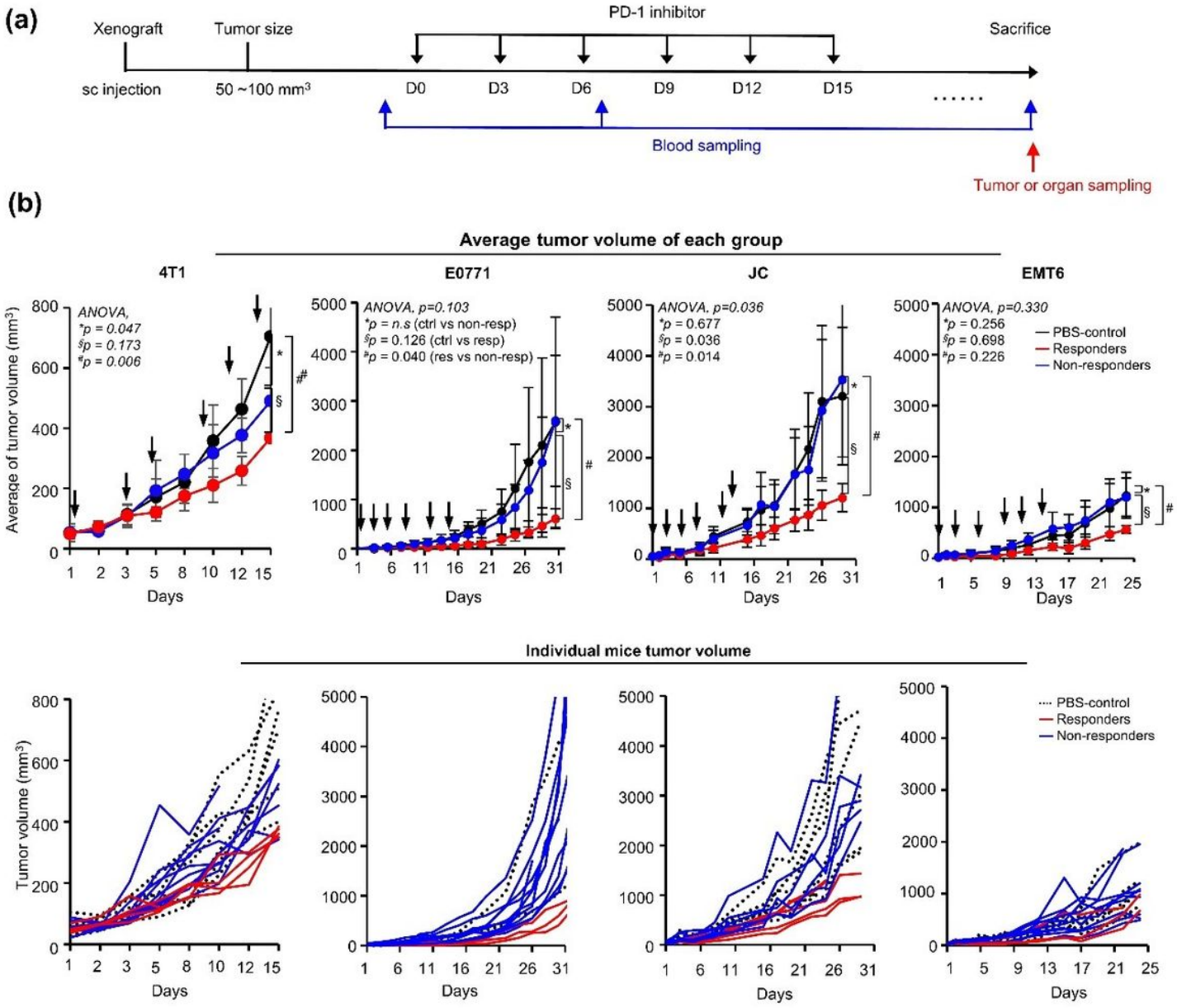

Figure 1

Efficacy of ICI in various TNBC syngeneic mice models. (a) Scheme of the in vivo efficacy test of ICI using syngeneic mice. 4T1, E0771, JC, and EMT6 cells were subcutaneously xenografted into 4-week-old female BALB/c mice and treated with PD-1 inhibitor by intraperitoneal injection every 3 days up to six times when tumors reached 50–100 mm^3 (black arrow). Peripheral blood samples were collected before injecting a PD-1 inhibitor, 7 days post of PD-1 inhibitor treatment, and at mice sacrifice (blue arrows). Tumor or organ samples were collected at the time of mice sacrifice (red arrow).

(b) The tumor growth inhibition curves of syngeneic mice (4T1, E0771, JC, and EMT6 xenograft model) in each group. Tumor growth inhibition curves were drawn as responders versus nonresponders. Black arrows indicate the time point of PD-1 inhibitor treatment. *p*-values were calculated using the ANOVA test (post hoc *p*-values; LSD). Data are presented as mean ± standard deviation. The black line indicates PBS

control, the red line indicates responders, and the blue line indicates nonresponders. The upper graph for the average value of tumor size based on responsiveness; the lower graph for tumor size of an individual mouse.

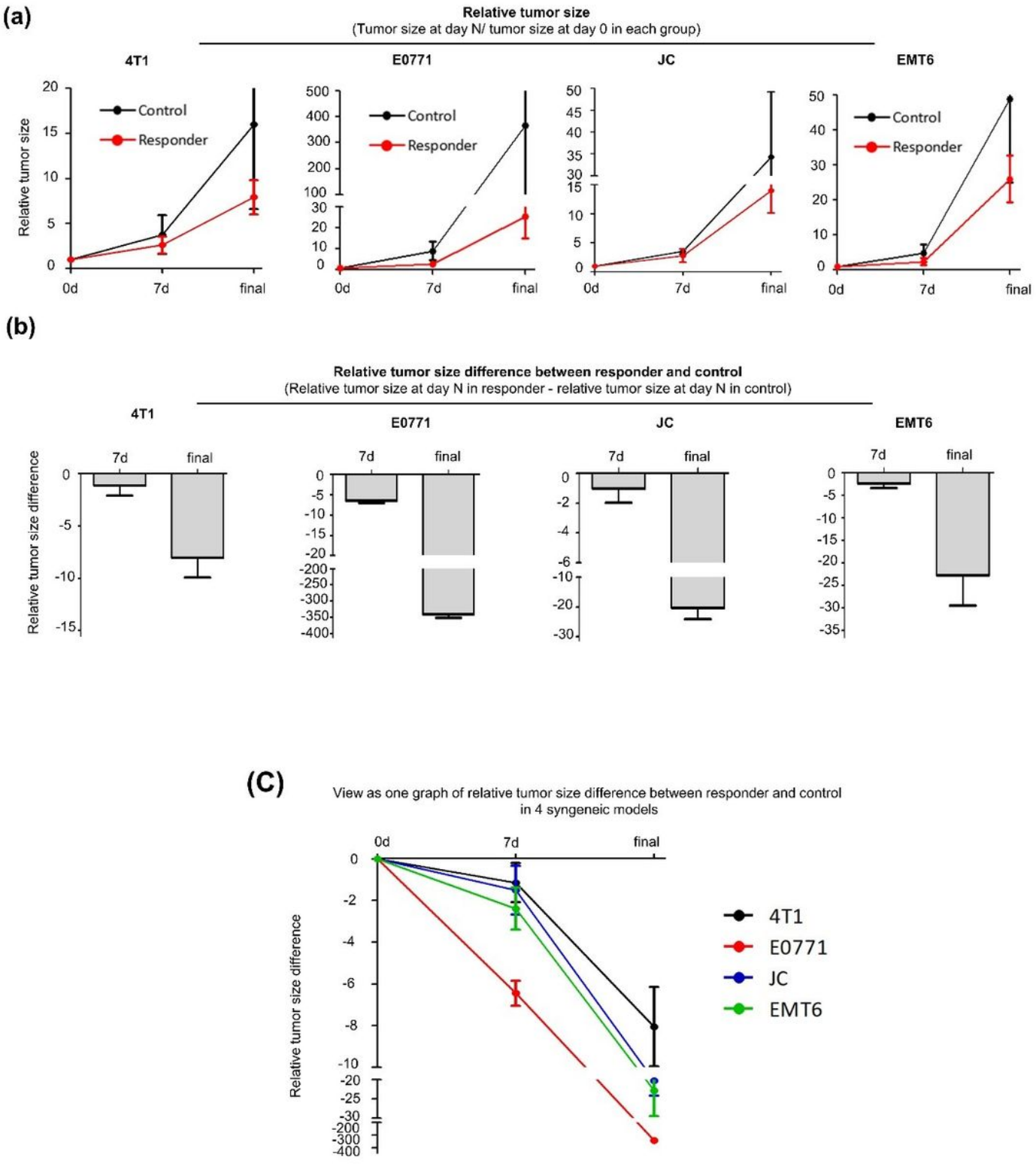

Figure 2

Early changes of tumor size predicted final efficacy of PD1 inhibitor treatment. (a) “Relative tumor size” was calculated by dividing tumor size at day N by the tumor size at day 0 in each group) in the control and responder group at 7 days post PD-1 inhibitor treatment and the final day just before sacrifice. Data are presented as mean ± standard deviation.

(b) “Relative tumor size difference between responder and control group” at 7 days post PD-1 inhibitor treatment and the final day, was calculated by subtracting relative tumor size at day N in control from the relative tumor size at day N in responder. Data are presented as mean ± standard deviation.

(c) To compare relative tumor size differences among 4 syngeneic models at 7 days post PD-1 inhibitor treatment and the final day, 4 separate bar graphs from each syngeneic model in Fig. 2b were transformed into one curved-line graph. Data are presented as mean ± standard deviation.

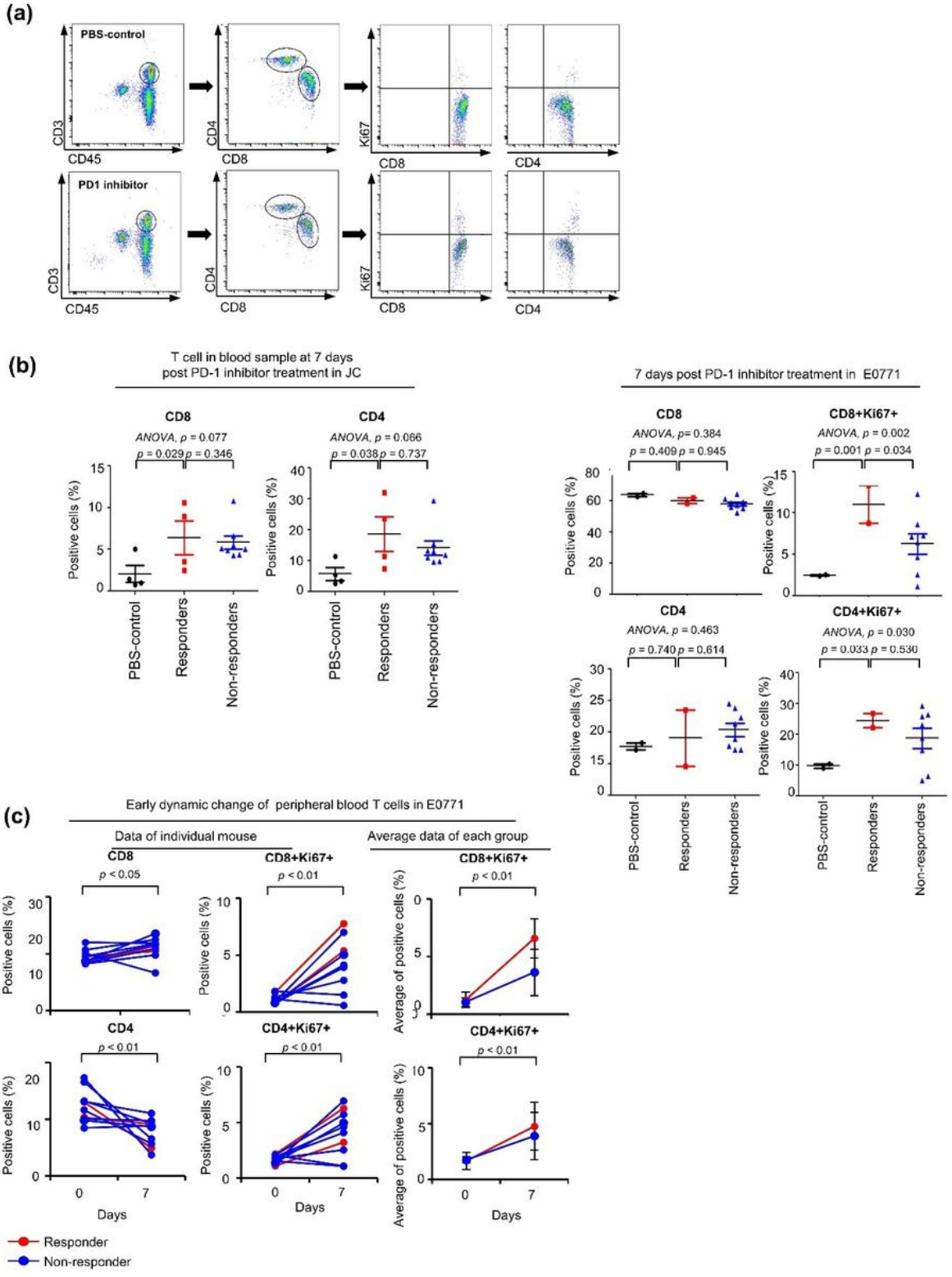

Figure 3

Early biomarker using peripheral blood T cells for the PD-1 inhibitor efficacy. (a) The gating strategy for flow cytometry analysis. Collected blood samples were stained with T cell markers, such as CD8 and CD4+ T cells and proliferation marker Ki67 and analyzed by flow cytometry. The *p*-values were calculated using the ANOVA test (post hoc *p*-values; LSD). Data are presented as mean ± standard deviation.

(b) Representative flow cytometry plots of peripheral blood CD8+ and CD4+ T cells at 7 days post-PD-1 inhibitor treatment. Responders showed higher CD8+ and CD4+ T cells compared to the control or nonresponders (JC model; left panel). Furthermore, responders also showed higher CD8+Ki67+ and CD4+Ki67+ cells compared to control or nonresponders (E0771 model; right panel). Black indicates PBS control, red indicates responders, and blue indicates nonresponders. *p*-values were calculated using Student's t-test or ANOVA test. Data are presented as mean ± standard deviation.

(c) The percent changes of CD8+ and CD4+ T cells and Ki67+ T cells of PD-1 inhibitor-treated mouse blood based on responsiveness from the pre-PD-1 inhibitor treatment to 7 days post-treatment. The average T cell-positive cells were then represented in each group. Red indicates responders, whereas blue indicates nonresponders. The *p*-values were calculated using Student's t-test. Data are presented as mean ± standard deviation.

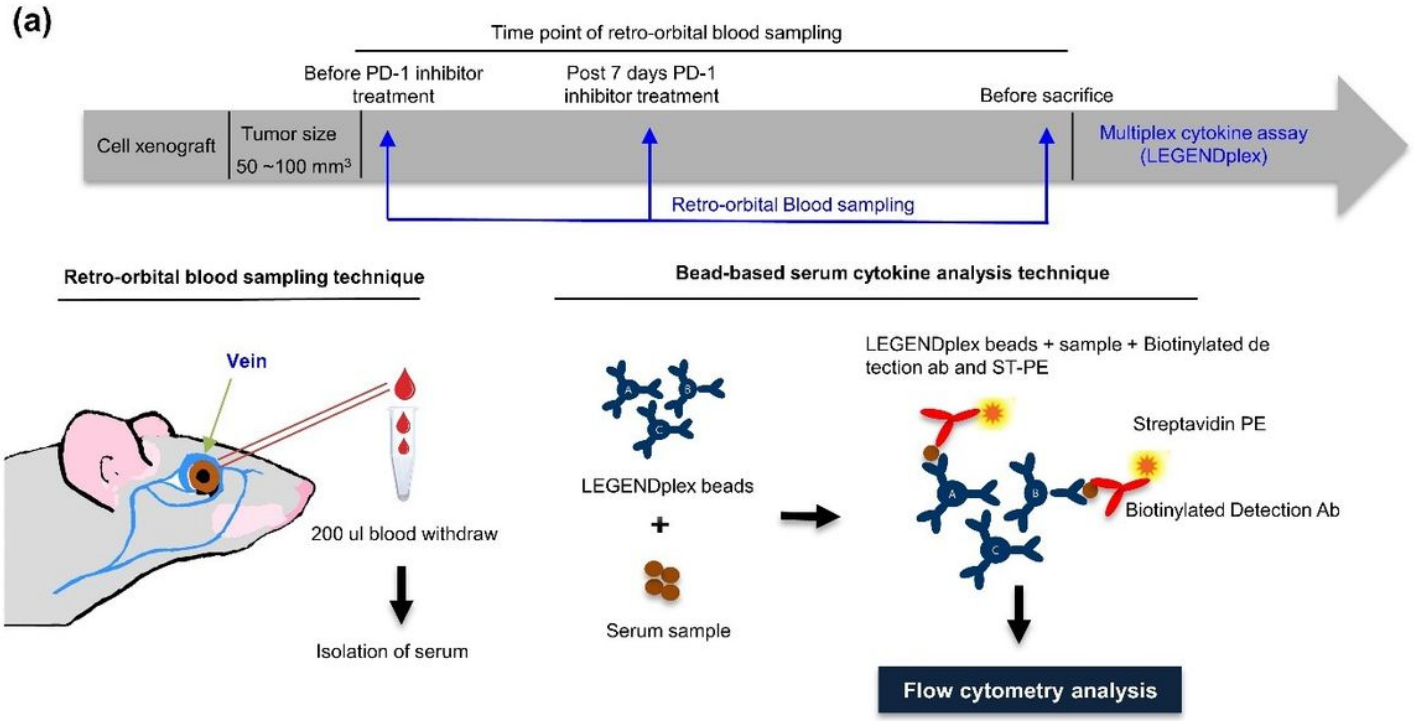

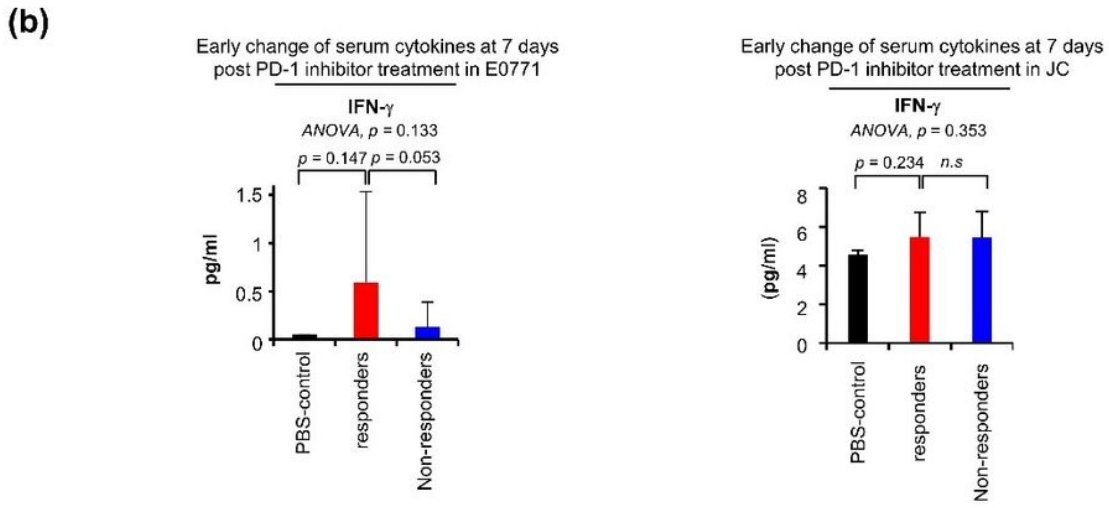

Figure 4

Early serum cytokine changes to predict PD-1 inhibitor efficacy. (a) Schematic diagram of how to do serum cytokine profiling in our mouse model, including time points of bleeding, retro-orbital blood collection technique and serum cytokine analysis technique of bead-based assay, LEGENDplex.

(b) The serum was separated from the blood at 7 days post-PD-1 inhibitor treatment. Multiple mouse cytokines (IFN-γ, TNF-α, IL-2, IL-6, and IL-10) were analyzed using a LEGENDplex bead-based immunoassay kit. The *p*-values were calculated using the ANOVA test (post hoc *p*-values; LSD). Data are presented as mean ± standard deviation.

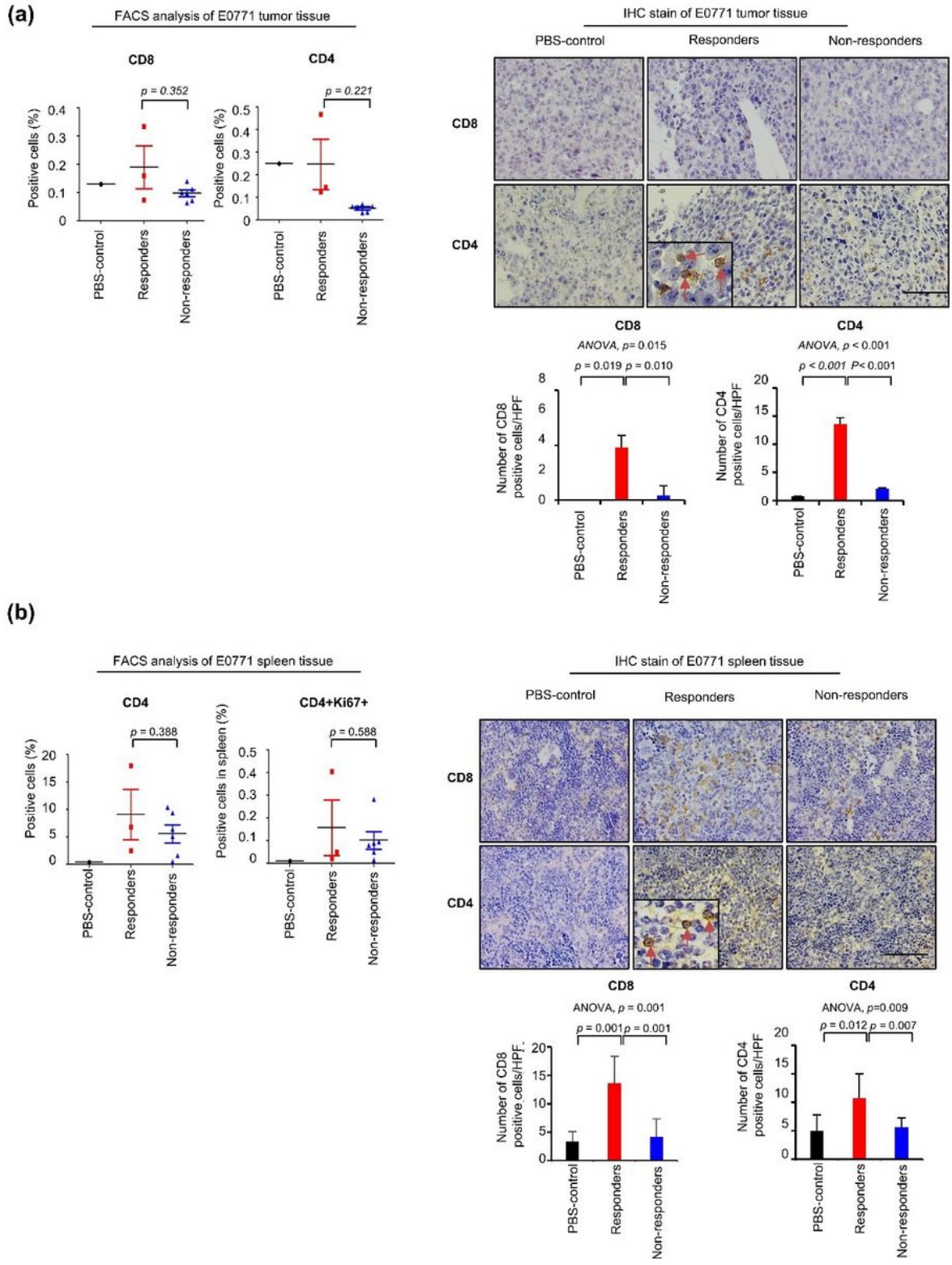

Figure 5

T cell infiltration in the tumor and proliferation in the spleen based on responsiveness after a PD-1 inhibitor treatment. Tumor infiltrating T lymphocytes (a) and T cell proliferation in the spleen (b) were analyzed with flow cytometry and IHC. (a and b) Dot plots represent the average numbers of CD8+ and CD4+ or CD4+Ki67+ T cells in the PBS control, responders, or nonresponders (left panel of a and b). The PBS-control graph has only one sample. It was not possible to calculate the *p*-value, so we just calculated

the *p*-value between the responder and nonresponder group by using the student;'s t-test. Data are presented as mean ± standard deviation. Representative IHC images in each group are shown, and bar graphs represent the average numbers of CD8+ and CD4+ T cells in each group in five random, nonoverlapped fields at ×400 magnification (right panels of a and b). The *p*-values were calculated using ANOVA test (post hoc *p*-values; LSD). Data are presented as mean ± standard deviation.

Supplementary Files

This is a list of supplementary files associated with this preprint. Click to download.

- Syngeneicprojectfinalsupplimentary.docx